CO_2−Ethanol Interaction Studied by Vibrational Spectroscopy in Supercritical CO_2

P. Lalanne,[†,‡] T. Tassaing,[†] Y. Danten,[†] F. Cansell,[‡] S. C. Tucker,[§] and M. Besnard*[,†]

Laboratoire de Physico-Chimie Moléculaire, CNRS (UMR 5803), Université Bordeaux I, 351 Cours de la Libération 33405 Talence Cedex, France, Institut de Chimie et de la Matière Condensée de Bordeaux, CNRS (UPR 9048), Château Brivazac, Université Bordeaux I, Av du Dr Schweitzer, 33608 Pessac Cedex, and Department of Chemistry, University of California, Davis, California 95616

Received: December 11, 2003; In Final Form: January 13, 2004

Infrared spectroscopic measurements of the ν_{OD} stretching vibration of dilute deuterated ethanol in supercritical CO_2 have been performed and analyzed, via a theoretical model and ab initio calculations, to better understand the ethanol−CO_2 interaction. It was found that strongly attractive interactions, predominantly due to dispersion, dominate the stabilization energy between ethanol and CO_2. Differences between the observed and theoretically predicted spectral shifts indicate the presence of local density enhancements. The continued observation of these enhancements up to temperatures significantly greater than the critical one, $T/T_c \geq 1.3$, suggests that ethanol is a strongly attractive solute for CO_2, at least in the spatial vicinity of the OH functional group. This suggestion is also supported by an analysis of the local density enhancement factors, as extracted from IR and other spectroscopies, as well as by the ab initio calculations.

1. Introduction

Fundamental research on intermolecular interactions and the structural and dynamic properties of condensed phases have been the main objective of many thorough works over the past thirty years.[1] These investigations typically focused on microphysical phenomena that occur over distances of several molecular layers and on time scales varying from femtoseconds to a few hundred picoseconds. The resultant development of theoretical concepts and experimental methods has now made it possible to obtain quantitative information about the structure and dynamics of molecules (solvation, chemical reactions) within dense media. More recently, such fundamental studies have been applied to the very interesting case of supercritical fluid environments (SCF),[2−4] which exhibit two important and interesting properties not present in liquid solvents.

The first unique property of SCFs is their variable densities, which can be changed continuously over all values between that of the liquid and that of the gas. As well, by working at temperatures only moderately greater than the critical temperature, it is possible to access a broad range of densities with only small changes in pressure and temperature. Working at these thermodynamic conditions is thus advantageous, as they can be used to establish a bridge between studies in the condensed phase and those in gas phase. This ability to control SCF densities is well known and has been frequently used in industrial applications to control the physical properties of a solvent and to allow, e.g., selective extraction of a solute from a dense matrix.[5]

The second, more specific, property of supercritical fluids is also related to the very high compressibility of a fluid in the region around its critical point. In this "compressible regime", the very high susceptibility of the solvent density to small variations of pressure generates strong density fluctuations at the microscopic level.[3,6,7] The presence of such microscopic density inhomogeneities in the solvent are then expected to have significant consequences for the structure and dynamics of a solute in such compressible SCF solutions. In particular, attractive solutes are expected to induce a region of local solvent density that can be greater than the density of the bulk solvent.[8,9] In addition, the extent of this density enhancement is, at least in part, driven by the relative strength of solute−solvent vs solvent−solvent interactions. However, the exact correlation of local density enhancements in supercritical fluids with the relative strength of the intermolecular interaction is still a matter of debate.[9−11]

Vibrational spectroscopy is a powerful tool for probing such questions about solute−solvent interactions since both the intensity and frequency associated with any vibrational mode of the solute depends on the potential of the mean force existing between the solvent and the solute.[12−14] Also, the solvent-induced forces that act along the solute vibrational coordinate may be separated into attractive and repulsive contributions. Consequently, if we vary the density of a SCF solvent over a broad range of values, we should observe strong variations in the intensity and frequency of the normal mode of the solute due to concomitant changes in the contributions of the attractive and repulsive solvent forces acting on the solute molecules.

Thus, the aim of the present paper is to assess the nature of, and balance between, the forces governing the intermolecular interaction between a supercritical solvent and a solute molecule by measuring the density-induced changes in a vibrational mode of the solute. In this article, we have focused our study on very dilute ethanol in supercritical CO_2. Not only is carbon dioxide the most common supercritical solvent, with easily accessible critical conditions, but supercritical CO_2 is widely used with ethanol as a cosolvent in industrial processes (fractionation, extraction, etc.) in order to enhance the solubility of polar and

* Author to whom correspondence may be addressed. Phone: 33 5 40 00 63 57. Fax: 33 5 40 00 84 02. E-mail: m.besnard@lpcm.u-bordeaux1.fr.
[†] Laboratoire de Physico-Chimie Moléculaire.
[‡] Institut de Chimie et de la Matière Condensée de Bordeaux.
[§] University of California, Davis.

10.1021/jp037802b CCC: $27.50
Published on Web 03/11/2004

high-molecular-weight solutes.[15−17] Fundamental research into the microscopic nature of the solvation process in this mixture will therefore provide highly desirable insights.

The OH stretching mode of the ethanol molecule has been measured by infrared absorption spectrometry to probe the intermolecular interactions. This vibration was selected because it can be considered as a vibrational mode of a pseudodiatomic molecule, and consequently, the evolution of its frequency shift with varying density can be analyzed using analytical models proposed in the literature.[18−20] The main advantage to using such statistical models to estimate the repulsive and attractive contributions to the solvent forces acting on the solute is that their application requires only basic molecular parameters, such as effective diameters, polarizabilities, and dipole and quadrupolar moments. It is noteworthy that very few vibrational spectroscopic studies have previously been undertaken on CO_2/alcohol mixtures under supercritical conditions. The focus of these studies was to measure the degree of hydrogen bonding of methyl alcohol-*d*[21,22] or ethanol-*d*[23] in supercritical CO_2 and to assess the equilibrium concentrations of the monomer and hydrogen-bonded species as a function of pressure and temperature. Moreover, these studies have also demonstrated the existence of a weak complex between CO_2 and alcohol.[24] These spectroscopic results lend support to previous thermodynamic investigations of CO_2/methanol[25] and CO_2/ethanol,[26] which have suggested the presence of a Lewis acid−base type of interaction in which the carbon atom of CO_2 and the oxygen atom of ethanol play the role of the electron acceptor and donor centers, respectively. This conclusion has also been further supported by ab initio studies of alcohol−CO_2 systems[27,28] and of the H_2O−CO_2 complex.[29,30] However, none of these studies provide a direct comparison between measured and calculated spectroscopic observables. The purpose of the present article is therefore 2-fold. First, it will provide a quantitative analysis of the spectroscopic observable by using an analytical model to determine the contributions of the repulsive and attractive forces acting between the ethanol and the CO_2 and to evaluate the weight of the different contributions, namely, dispersion, induction, and dipole−quadrupole to the attractive part of the intermolecular potential. The second purpose is to compare these results with predictions from ab initio calculations.

The present paper is organized as follows. Section 2 provides the theoretical background for the Buckinghan−Ben-Amotz model, while section 3 provides the experimental details. In section 4.1, we present the infrared spectra of the ν_{OD} stretching mode of deuterated ethanol diluted in CO_2 measured along three isotherms in the density range 0.03−0.7 g cm^{-3}. These experimental data are analyzed in section 4.2 by using the Buckingham−Ben-Amotz model to estimate the contributions of the repulsive and the attractive (dispersion, induction, dipole/quadrupole) forces to the ν_{OD} stretching frequency. Then, in section 4.3, the departure of the experimentally determined spectral shifts from the linear behavior predicted theoretically for these shifts in a homogeneous fluid as a function of increasing pressure (in section 4.2) are analyzed in terms of local density enhancements. Finally, the last section, 4.4, is devoted to the study of the CO_2−ethanol interaction on the basis of results derived from the analytical approach and also from ab initio calculations for an isolated CO_2−ethanol pair. Conclusions follow.

2. Theoretical Background

We briefly present the basic theoretical background for vibrational frequency shift calculations that have been given previously in detail in the literature. The interpretation of the frequency shifts, $\Delta\nu$, is based on the Buckingham−Ben-Amotz approach.[19,20,31] According to this theory, the frequency shift of an anharmonic stretching vibration of a solute diluted in a solvent is a sum of two contributions

$$\Delta\nu = \Delta\nu_R + \Delta\nu_A \tag{1}$$

The former contribution, $\Delta\nu_R$, represents the frequency variation due to repulsive forces between the solute and the solvent. The latter term, $\Delta\nu_A$, represents the frequency variation due to attractive forces.

The Repulsive Contribution. The calculation of the repulsive contributions to the frequency shift $\Delta\nu_R$ is based on a "perturbed hard fluid model" developed by Ben-Amotz and Herschbach.[18,32] According to this model, the solute molecule is approximated by a pseudodiatomic molecule comprised of two hard spheres of diameter σ_1 and σ_2 located a distance r_{12} apart and immersed at infinite dilution in a solvent of hard spheres of diameter σ_S and density ρ.

The repulsive shift $\Delta\nu_R$ is then given by

$$\Delta\nu_R \approx \nu_0 \frac{F_R}{f}\left[-\left(\frac{3g}{2f}\right) + \left(\frac{G_R}{F_R}\right)\right] \tag{2}$$

where ν_0 is the unperturbed vibrational frequency of the isolated solute molecule, f and g are the intramolecular harmonic and anharmonic force constants, respectively, and F_R and G_R are the linear and quadratic coefficients in an expansion of the potential of mean field along the pseudo-diatomic bond of the solute molecule.

The Attractive Contribution. The calculation of the attractive contribution to the frequency shift, $\Delta\nu_A$, is based on the van der Waals mean-field approximation developed by Chandler and co-workers.[14] This contribution is proportional to the density ρ of the solvent according to

$$\Delta\nu_A = C_A\rho \tag{3}$$

The constant C_A can be calculated using the simple long-range solvation attractive-forces model. Considering attractive solvation forces that arise from dispersive, inductive, and dipole−quadrupole interactions, the angle-averaged attractive potential energy V_A between the solute (O) and the solvent molecule (S) can be expressed as the sum of three terms, namely

$$V_A = V_{dispersion} + V_{induction} + V_{dipole-quadrupole} \tag{4}$$

where

$$V_{dispersion} \approx -\frac{3}{2}\left(\frac{I_0 I_S}{I_0 + I_S}\right)\left(\frac{\alpha_0\alpha_S}{r_{0S}^6}\right) \tag{5}$$

$$V_{dipole-quadrupole} \approx -\frac{1}{k_B T r_{0S}^8}(\mu_0^2\,\theta_S^2 + \mu_S^2\,\theta_0^2), \tag{6}$$

$$V_{induction} \approx -\frac{1}{r_{0S}^6}(\mu_0^2\alpha_S + \mu_S^2\alpha_0) \tag{7}$$

and α_i, μ_i, I_i, θ_i, r_{0S} are, respectively, the polarizability, the dipole moment, the potential of ionization, the quadrupole moment, and the distance between the center of masses of the pseudodiatomic solute and the solvent.

These expressions can be used to derive the attractive mean-field parameter C_A

$$C_A = A_{\text{dispersion}} + A_{\text{induction}} + A_{\text{dipole}-\text{quadrupole}} \quad (8)$$

where

$$A_{\text{dispersion}} \approx -\frac{4\pi}{3}\frac{1}{\sigma_a^3}\left[\frac{3}{2} I_a \frac{\partial \alpha_0}{\partial Q}\Delta Q\right]\alpha_S \quad (9)$$

$$A_{\text{induction}} \approx -\frac{4\pi}{3}\frac{1}{\sigma_a^3}\left[2\mu_0 \frac{\partial \mu_0}{\partial Q}\Delta Q\right]\alpha_S - \frac{4\pi}{3}\frac{1}{\sigma_a^3}\left[\frac{\partial \alpha_0}{\partial Q}\Delta Q\right]\mu_S^2 \quad (10)$$

$$A_{\text{dipole}-\text{quadrupole}} \approx -\frac{4\pi}{3}\frac{1}{\sigma_a^5}\left[\frac{2}{k_B T}\theta_0 \frac{\partial \theta_0}{\partial Q}\Delta Q\right]\mu_S^2 - \frac{4\pi}{3}\frac{1}{\sigma_a^5}\left[\frac{2}{k_B T}\mu_0 \frac{\partial \mu_0}{\partial Q}\Delta Q\right]\theta_S^2 \quad (11)$$

and Q is the normal coordinate of the solute vibrational mode, ΔQ is the variation of the normal mode coordinate upon vibrational transition, and

$$\sigma_a \equiv \frac{1}{2}(\sigma_0 + \sigma_S) \quad \text{and} \quad I_a \equiv \left(\frac{I_0 I_S}{I_0 + I_S}\right)$$

3. Experimental Details

The measurements were performed on a Biorad interferometer (type FTS-60A) equipped with a globar source, a KBr beam splitter, and a DTGS detector. Single-beam spectra recorded in the spectral range 400−6000 cm^{-1} with a 2-cm^{-1} resolution were obtained by Fourier transformation of 50 accumulated interferograms.

We used a special inconel cell having two cylindrical silicon windows and a path length of 25 mm. Details of the optical cell have been presented previously in reference.[16] The sealing is obtained using the unsupported-area principle. The windows are positioned on the flat surface of the inconel plug. A 100-μm Kapton foil placed between the window and the plug compensates for any imperfections between the two surfaces. Flat Teflon seals ensure that the plug and the cell body are well sealed. Heating is performed by four cartridge heaters dispersed throughout the body of the cell in which two thermocouples were placed. The first thermocouple is located close to one cartridge to enable accurate temperature control, while the second is located close to the sample area in order to ensure good temperature regulation, with an accuracy of about $\Delta T \approx \pm 0.5$ °C. The cell was connected via a stainless steel capillary to a hydraulic pressurizing system that allows the pressure to be raised to 50 MPa with an absolute uncertainty of ±0.1 MPa and a relative error of ±0.3%. The cell was filled with deuterated ethanol (Prolabo product, 99.9% purity) at the concentration of 6×10^{-3} mol L^{-1} and heated to the required temperature. The CO_2 ("Air Liquide" company) was then added up to the desired pressure.

4. Results and Discussion

4.1. Infrared Spectra of Ethanol Diluted in CO_2. The strong absorption of the combination band of CO_2 precludes clear observation of the OH stretching vibration in the spectral range between 3000 and 4000 cm^{-1}. To circumvent this drawback, we have used deuterated ethanol (CH_3CH_2OD). The spectra of the OD stretching region have been collected at three different constant temperatures, T = 40, 80, and 120 °C, as a function of pressure, from 1 to 35 MPa, for the CO_2/ethanol mixture. Typical infrared spectra, as they appear after the removal of the CO_2 contribution, are displayed in Figure 1 for T = 120 °C. The ν_{OD} stretching mode of the ethanol monomer is observed at 2700 cm^{-1}. This assignment is supported by the absence of any broad spectral band, due to aggregated species, on the low-frequency side of ν_{OD}. This assignment is also consistent with the high dilution of the mixture considered. As the pressure increases, there is a strong modification of the band shape as it evolves from the vibrational−rotational *P*,*Q*,*R* structure observed at low pressure to the Lorentzian type of profile observed at high pressure (Figure 1). The evolution of the band shape is accompanied by both a redshift of the band center position and an increase in the band intensity. The evolution of both the integrated extinction coefficient, $\bar{A}$, and the frequency shift, ν_{OD}, of the ethanol monomer vibrational band is shown in Figures 2 and 3 as a function of density.

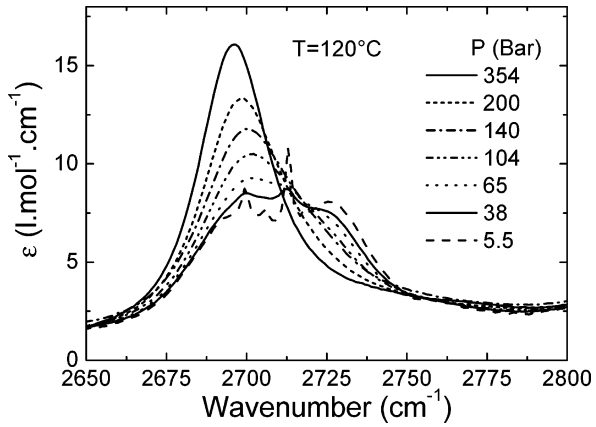

Figure 1. Infrared spectra in the OD stretching region of deuterated ethanol highly diluted ([CH_3CH_2OD] = 6×10^{-3} mol L^{-1}) in supercritical CO_2 as a function of pressure at T = 120 °C.

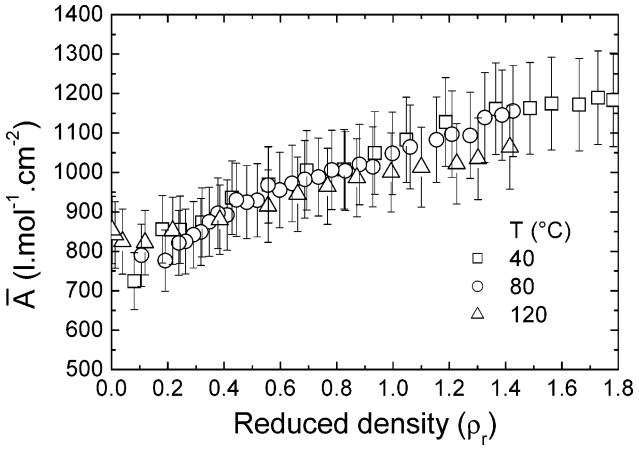

Figure 2. Evolution of the integrated intensity (molar extension coefficient) of the ν_{OD} band of deuterated ethanol as a function of the density of supercritical CO_2.

At low density, the integrated extinction coefficient $\bar{A}$ is independent of the temperature and is found to be about 800 ± 50 L mol^{-1} cm^{-2}. To the best of our knowledge, this value has not been reported in the literature for gaseous ethanol. However, it is in agreement with that reported for methanol,[33] which was found to be 980 L mol^{-1} cm^{-2}. With increasing pressure, we observe an increase of the integrated area up to a value of about 1200 L mol^{-1} cm^{-2} (cf. Figure 2). The integrated extinction coefficient $\bar{A}$ of a vibrational transition is related to the transition

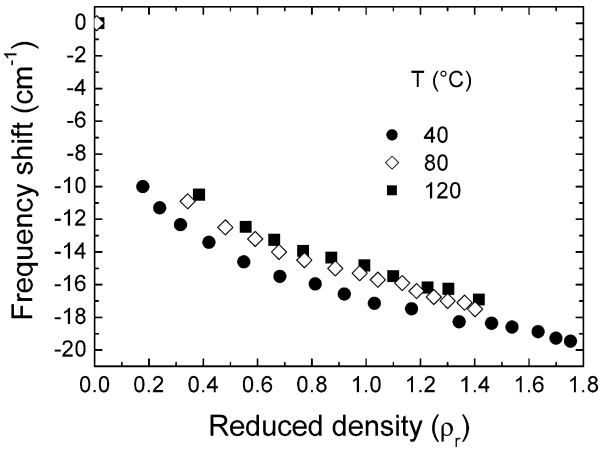

Figure 3. Evolution of the band-center frequency of the ν_{OD} band of ethanol as a function of the density of supercritical CO_2 along three isotherms.

moment ($\partial\vec{\mu}/\partial q$) according to the relation

$$\bar{A} = \int_{\text{band}} \epsilon(\bar{\nu})\, \mathrm{d}\bar{\nu} = \frac{1}{2.3}\frac{\pi N_{\text{av}}}{3c^2\mu_{\text{red}}}\left(\frac{\mathrm{d}\vec{\mu}}{\mathrm{d}q}\right)^2_{q=0}$$

where μ_{red} is the reduced mass of the oscillator. This expression, which involves only molecular properties, shows that the integrated extinction coefficient should be density independent. This prediction is in marked contrast with the experimental observation which shows that $\bar{A}$ increases by about 50% as the reduced density $\rho_r = \rho/\rho_c$ of CO_2 (where ρ_c is the critical density of CO_2) increases from 0 to about 1.8, independent of the temperature. Therefore, the transition moment itself is sensitive to the solvent density.

In the same range of density, the band center frequency of this mode shows a nonlinear redshift that weakens slightly with increasing temperature (cf. Figure 3). From these observations, it can be inferred that the ethanol interacts with the surrounding CO_2 molecules.

4.2. Frequency-Shifts Calculations. To assess the nature of the solute−solvent interactions that give rise to the evolution of the band center frequency of the OD stretching mode with pressure, we have used the analytical model presented in section 2 to predict the frequency shift of the ν_{OD} vibration as a function of the reduced density. The parameters used in this model were extracted from both literature data and ab initio calculations and are reported in Table 1. The results of the calculation at $T = 40$ °C are compared with the experimental data in Figure 4. Examination of this figure shows that the shifts of the band center due to the repulsive forces are positive (blueshift) and increase with the density. The calculated values of this quantity, which do not exceed 1 cm^{-1} at reduced densities, ρ_r , less than 1, grow slightly faster at higher densities, but still only reach modest values of less than 5 cm^{-1} at densities as high as that characteristic of the liquid, $\rho_r = 2.5-3$. In contrast, the shift due to the attractive forces is negative and varies markedly with density in a linear way (as expected according to the model (see paragraph 2)). At each density, the magnitude of the calculated values are always much greater than those due to the repulsive forces. Therefore, the shift of the band center, which is governed by the balance between repulsive and attractive interactions, is always found to be at lower frequencies, indicating that attractive forces play the major role in the density range investigated.

This theoretical prediction is in qualitative agreement with the experimentally observed trend (Figure 4). However, the calculated values disagree quantitatively with experimental ones in the reduced density range 0.04−1.5. One may argue that the theoretical approach used, which models the vibrational mode of a polyatomic solute as the stretching vibration of a diatomic molecule, is certainly crude. However, it is important to recognize that the discrepancies between calculated and experimental shifts are observed at densities around the critical density for $\rho_r < 1.3$, i.e., in that range usually called the "compressible regime" of the fluid where density inhomogeneities are expected, whereas much better agreement is attained at both high and very low densities. This suggests that the nonlinear behavior of the shift observed in this density region may be directly related to the local density enhancements (LDE) expected around attractive solutes in solutions close to the critical point.[3,4,34,35] It is important to recall that studies in UV−vis spectroscopy[3,4,36,37] have reported that the spectral shifts associated with the electronic transition of a highly dilute chromophore in an SCF exhibit a marked deviation from linearity when the reduced density varies in the approximate range $0.2 < \rho_r < 1.2$. These deviations have been interpreted to mean that the local density around the solute is in excess of that of the bulk fluid, i.e., of the homogeneous fluid under the same temperature and pressure conditions, thus signifying the presence of LDEs.

The general validity of such enhanced local-density-based interpretations of this type of nonlinear behavior has been well established by numerous computer simulations studies, which

TABLE 1: Molecular Parameters[a]

solute CH_3CH_2OD	
M (g mol^{-1})	47
r_0 (Å)	0.967[b]
r_{eff} (Å)	1.98[b]
σ_{solute} (Å)	4.63[c]
σ_1 (Å)	4.41[c]
σ_2 (Å)	2.4[c]
μ (D)	1.69[d]
α (Å^3)	5.11[e]
θ (D Å)	5.7[b]
ν_0 (cm^{-1})	2713[f]
dα/dr (Å^2)	13.3[b]
dμ/dr (D.Å^{-1})	1.16[b]
f (dyn cm^{-1})	9.22 0.10^5 [b]
g (dyn cm^{-2})	-1.294×10^{14} [g]
I_{solute} (cm^{-1})	84654[d]
Δr (Å)	0.0123
solvent CO_2	
μ (D)	0
σ_s (Å)	3.96[c]
I (cm^{-1})	111000[d]
α (Å^3)	2.6[e]
θ (D Å)	−4.49[e]

[a] Key: M, molar mass; r_0, O−H bond length; r_{eff}, effective diatomic separation between the center of mass of the two groups associated to the diatomic oscillator, namely, C_2H_5O (1) and H (2)(see ref 19); σ_{solute}, solute diameter; σ_{solvent}, solvent diameter; σ_1 and σ_2, effective diameters of the two spheres of the diatomic oscillator calculated from van der Waals volume; I, ionization energy; μ, dipole moment; α, polarizability; θ, quadrupolar moment; ν_0, gas-phase Q branch frequency; dα/dr and dμ/dr, polarizability and dipole moment derivatives; f and g, harmonic and anharmonic force constants. $\Delta r = -3/2hc\nu_0 g/f^2$.[19] [b] Calculated by ab initio[28] using the Moller−Plesset perturbation theory at the second-order level (MP2) with the Dunning's aug-cc-pVDZ basis set. [c] Calculated by the method of Bondi.[50] [d] From CRC Handbook of Chemistry and Physics, 61st edition, CRC Press, Inc. [e] From ref 51. [f] From the experimental gas-phase Q branch frequency. [g] g has been calculated using the following expression: $\omega_e x_e = 3h/(32\pi^4\mu_{\text{red}}{}^2c^3\omega_0)(-5g^2/(16\pi^2\mu_{\text{red}}c^2\omega_0{}^2) - j)$ for the intramolecular potential V of the vibrator given by $V = (1/2)fq^2 + (1/2)q^3 + jq^4$. The anharmonic constant $\omega_e x_e$ for gaseous deuterated ethanol has been found experimentally to be equal to 50 cm^{-1}.

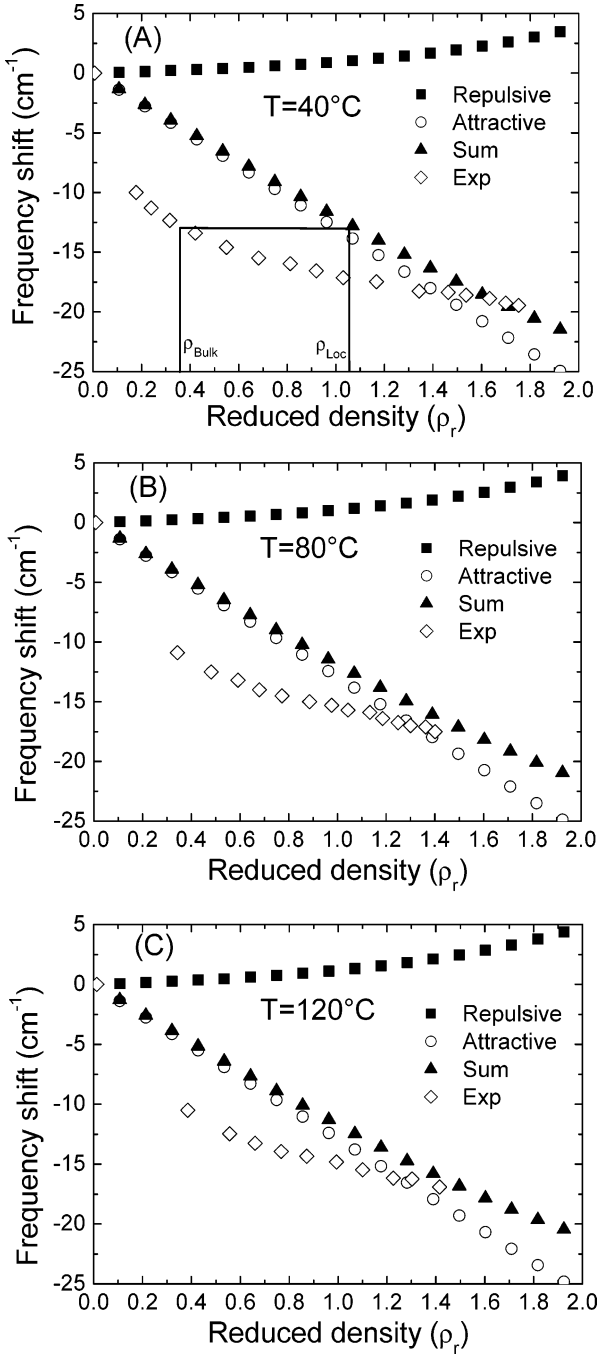

Figure 4. Comparison between the experimental and the calculated frequency shifts at $T = 40$ °C (A), $T = 80$ °C (B), and $T = 120$ °C (C).

have confirmed and explained the presence of such local density enhancements in compressible SCFs.[3,34,10,11] Similar nonlinear discrepancies between predicted and experimental values have been observed in three previous studies of vibrational shifts in SCFs,[38,39,40] although in only one of these studies did the authors attribute their observations to LDEs.[40,41] However, theoretical and simulation work on vibrational spectroscopy in SCFs has since shown that, for attractive solute−solvent systems in compressible SCFs, LDEs should be expected to give rise to nonlinear deviations of the vibrational shifts away from those predicted in the absence of such density enhancements, just as they do for electronic spectral shifts.[34,42] Both the results presented herein, as well as other work in progress in this laboratory on several other organic solutes dissolved in supercritical CO_2, confirm this expectation. In particular, the good quantitative agreement between the experimental shifts and the theoretical predictions at both very low and high reduced densities for all temperatures considered (parts A−C of Figure 4), with the nonlinear deviations occurring only at intermediate reduced densities, is consistent with the trends expected when LDEs are involved. The fact that the magnitude of the observed nonlinear deviations decrease with increasing temperature is also consistent with the expected behavior of LDEs, that is, with a reduction in the presence of such enhancements as one moves away from the critical point (increasing temperature). However, while this general decrease in the degree of nonlinear behavior with increasing temperature is expected, the rate of this decrease is here much less rapid than has typically been observed.[3,4] Specifically, in electronic spectral shift studies, LDE-based nonlinear behavior has typically been confined to temperatures below $T_r \approx 1.1$ or lower, while in the present vibrational spectral shift studies, such nonlinear deviations are still present even at the highest temperature considered (Figure 4C), 80 °C, which corresponds to a reduced temperature of $T_r = 1.3$. We will present a hypothesis explaining this result below.

4.3. Analysis of the Local Density Enhancement. From the evolution of the frequency shift as a function of the density, it is possible to extract a local density enhancement factor, $\Delta\rho = \rho_{loc} - \rho_{bulk}$, which reflects the difference between the local solvent density in the solvation sphere of ethanol, ρ_{loc}, and the density of the bulk solvent, ρ_{bulk}. However, there are no theoretical methods available for determining ρ_{loc}, and we have therefore resorted to the empirical method frequently used in the spectroscopic work in the literature. For this purpose, we have assumed that the frequency shifts calculated previously using the Buckingham−Ben-Amotz approach provides a good prediction of the transition frequency shift in a homogeneous fluid. The method used to evaluate ρ_{loc} from the Buckingham−Ben-Amotz reference line is illustrated in Figure 4A. From ρ_{loc} we then compute $\Delta\rho$, at each state point considered. The resulting variation of the local density enhancement factor $\Delta\rho$, reported in Figure 5, appears as a broad curve that exhibits a maximum at a reduced density of about $\rho_r \sim 0.4$. This curve has the same characteristic appearance as those reported in the literature from UV−vis spectroscopic measurements.[36,37] Moreover, the value of the density maximum falls in the same approximate range, $0.35 < \rho_r < 0.5$, as do those reported in many other studies of LDEs.[3,9] For comparison, we have also displayed in Figure 5 the values of the excess local density extracted from NMR measurements of chemical shifts of the hydroxyl proton of the ethanol molecule in the CO_2/ethanol system at $T_r = 1.03$ (40 °C).[43] These NMR results appear to be qualitatively, but not quantitatively, in agreement with those predicted by our vibrational shift data. The qualitative similarity strongly suggests that local density enhancements are indeed responsible for the nonlinear behavior of the IR band shift observed in the present work. Also, the quantitative differences in the extracted values of these enhancements should not be considered to detract from this conclusion, since IR and NMR spectroscopies are probing different molecular properties and would thus be expected to exhibit different sensitivities to the presence (and the exact nature) of LDEs. Indeed, differing LDE predictions for the same system when examined by differing spectroscopies has previously been observed, e.g., by Heitz and Maroncelli.[44]

We now address the question of how the observed differences between the LDE values extracted from the IR and NMR spectra of the ethanol/CO_2 system can be interpreted. Also, we ask whether we can also understand the observation that the IR

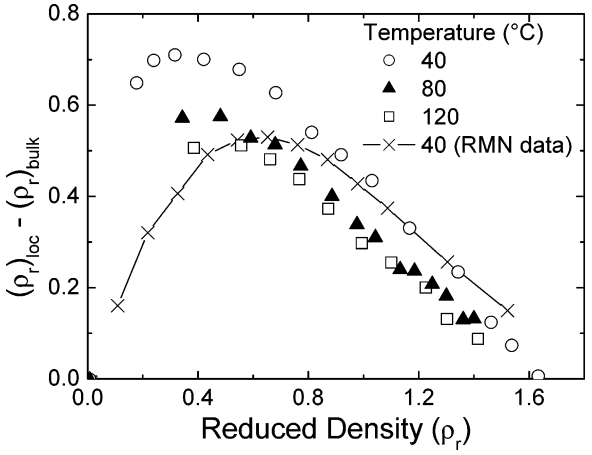

Figure 5. Evolution of the local density enhancement factor as a function of the density of supercritical CO_2 for the three temperatures investigated. The crosses indicates the NMR results reported in the literature for ethanol diluted in supercritical CO_2 at $T = 40$ °C.[43]

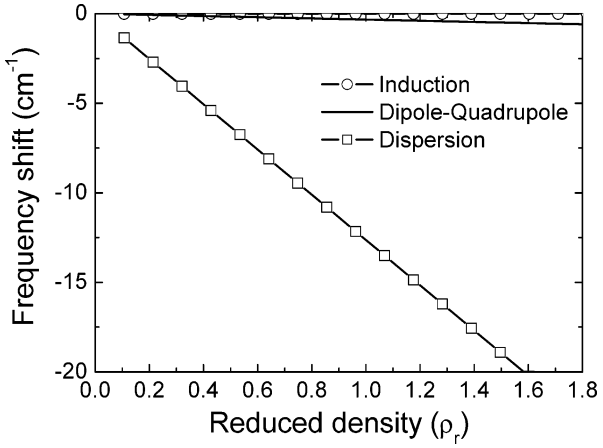

Figure 6. Relative energetic contributions in the attractive part of the frequency shift.

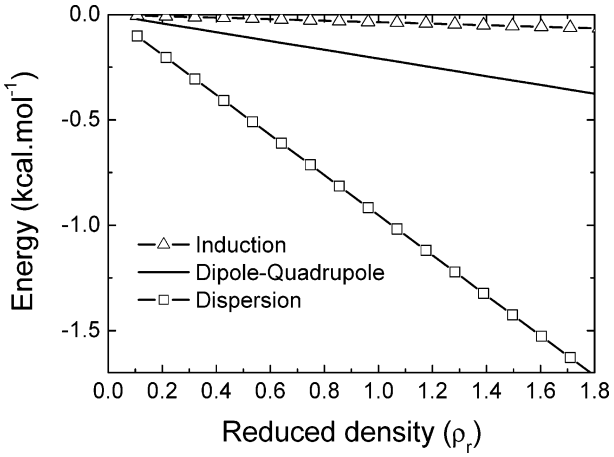

Figure 7. Relative weight of the different energetic contribution.

spectra reflect the presence of LDEs to unusually high values of the temperature. To begin, we recognize that, as will be shown below, the vibrational shift is dominated by the short-range dispersion interactions (r^{-6}) between ethanol and CO_2, being nearly insensitive to the presence of the dipole−quadrupole interactions. In contrast, the analysis of the NMR shifts presented in ref 43 suggests that the quadrupolar field of the CO_2 solvent generates a significant, longer-range term (r^{-4}) in the NMR shift expression. It therefore seems reasonable to assume that the IR experiments probe the nature of the solvent density over a shorter range (smaller local region) than do the NMR experiments. Simulations studies have shown consistently that a decrease in the local range around the solute over which the solvent density is considered will lead to an increase in the predicted value of the LDE, a result which follows directly from the fact that solvent density enhancements fall off with distance as one moves away from an attractive solute.[3,10] Thus, since IR probes a shorter range than does the NMR technique, the IR shifts would be expected to "feel" greater local densities than do the NMR shifts, and this is exactly the result observed in Figure 5, where the IR results suggest the presence of larger LDEs than do the NMR results. Additionally, Goodyear et al. have shown that when the local range is decreased, potential-induced contributions to the LDEs, which tend to be maximized at low bulk densities, play a greater role.[10] Consequently, as the range of the local region is decreased, the position of the maximum in $\Delta\rho$ vs ρ_r is expected to shift to lower values of ρ_r, exactly as observed in Figure 5 when one compares the shorter-range IR-based LDEs with the longer-range NMR-based LDEs.

The presence of LDEs in the IR results up to temperatures as high as $T_r = 1.3$ is somewhat harder to rationalize, as such results have tended to be observed only for very strongly attractive solute/solvent systems.[3] However, because IR shifts tend to probe only over a very short range, such as a single solvation shell, the presence of even a very small number of excess solvent molecules in this shell, e.g., 1 or 2, could generate a noticeable enhancement of the local density in this small region. Consequently, if there is a tendency for any sort of complexation between the solute OD dipole and one or more CO_2 molecules, one might observe the LDE signature in the IR spectra at higher than normal temperatures. That such "complexations," i.e., strongly asymmetric-enhanced local densities, may exist under supercritical conditions is supported by several computer simulation studies of SCFs.[45−47] We therefore turn our attention to the ethanol−CO_2 interaction to ascertain whether the presence of extra CO_2 molecules around the OD functional group is likely. As we shall see below, the OD group seems to be particularly sensitive to the presence of excess CO_2 molecules in the local region, resulting in the formation of an electron-donor−acceptor (EDA) complex. This complexation generates an IR shift, thus potentially increasing the temperature range over which LDEs would be observed.

4.4. Analysis of the Ethanol−CO_2 Interaction. *From Analytical Calculations.* To examine the relative contribution of the different mechanisms involved in the attractive interaction existing between ethanol and the CO_2, we have calculated the contribution of the different solute−solvent interaction mechanisms to the OD vibrational shift by evaluating the expressions eq 9−11 with the values of the parameters reported in Table 1. The results, shown in Figure 6 for $T = 40$ °C, demonstrate that the contribution of the dispersive term overwhelmingly dominates the observed frequency shift. We emphasize, however, that this result applies only to the vibrational spectra, and it should not be misconstrued to mean that only dispersive forces contribute to the stabilization of the CO_2/ethanol interaction. On the contrary, an estimate of the relative weights of the different contributions to the attractive part of the intermolecular potential, which was calculated from eqs 5−7 with the parameters of Table 1 for $T = 40$ °C and is shown in Figure 7, illustrates that the dipole−quadrupole interaction plays a significant role in the stabilization of the CO_2/ethanol interactions, although it is only about one-fourth that of the dispersive contribution. A comparison of eqs 6 and 11 shows that the lack of importance of the dipole−quadrupole term in the spectro-

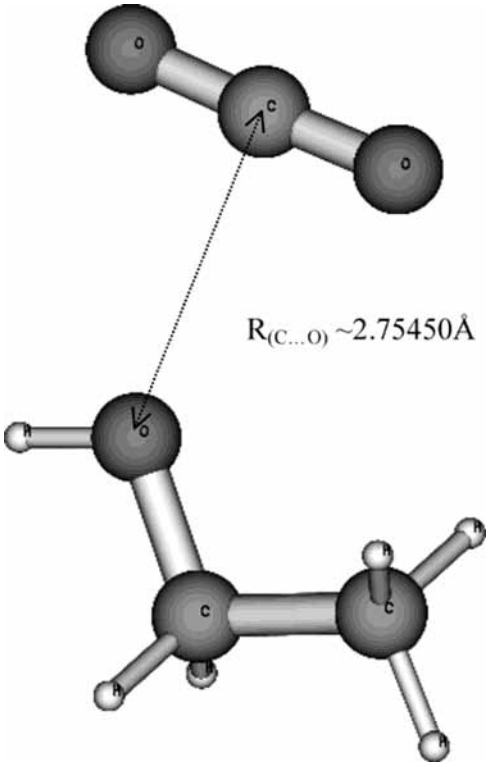

Figure 8. Optimized geometry of the CO_2/ethanol complex.

scopic shift arises because the shift is computed from a derivative quantity which reflects not the magnitude of this component of the energy, but rather, how much it changes with variations of the vibrational normal coordinate, *Q*. Finally, we also note that the energy associated with the dipole−quadrupole mechanism of interaction is inversely proportional to temperature and thus that its contribution will tend to vanish with increasing temperature.

From ab initio Calculations. To gain additional insight into the origin of the interaction between ethanol and CO_2, we performed ab initio calculations using the Gaussian suite of programs.[48] The details of these calculations have been reported elsewhere, so we will recall here only the most relevant findings.[28] Specifically, the geometry of an isolated CO_2/ethanol pair was fully optimized using second-order Moller−Plesset perturbation theory (MP2) using Dunning's aug-cc-pVDZ basis set. The resultant equilibrium geometry, having C_s symmetry shown in Figure 8, was found to have an intermolecular distance of $R_{(C\cdots O)}$ of 2.754 Å and intermolecular angle of $\alpha_{H-O\ldots C}$ of 114.702°. This complex was found to result from an EDA interaction in which the carbon atom of the CO_2 molecule acts as a Lewis acid and the oxygen atom of ethanol plays the role of electron donor center. The interaction energy of the complex was determined to be −2.96 kcal mol^{-1}, after correcting for basis-set superposition error.[49] Moreover, it was also found that the contribution of electron-correlation effects to the stabilization energy, which can be thought of as the dispersion contribution to this energy, is significant, having a value of about −1.3 kcal mol^{-1}. These ab initio results, then, clearly support our hypothesis, made above, that a relatively strong, specific interaction exists between the OD functional group and CO_2 and thus that such an interaction is most likely responsible for the difference between the LDEs predicted from the OD vibrational shifts presented here and those predicted from other spectroscopies.

Finally, we were also interested in the vibrational analysis of the internal modes of the CO_2/ethanol complex and, more particularly, in the perturbations induced by EDA interaction on the characteristic infrared and Raman frequencies and intensities. In particular, we found that the ν_{OH} stretching mode of ethanol interacting with a CO_2 molecule is shifted to lower frequencies by about 5 cm^{-1} compared to that calculated for the isolated ethanol molecule. Moreover, because of this interaction, the integrated intensity of this mode increases by a factor of 1.6. These two observations are consistent with the infrared experimental results reported on Figures 2 and 3.

5. Conclusion

The infrared spectra of the ν_{OD} stretching vibration of deuterated ethanol diluted in supercritical CO_2 have been measured along three isotherms in the reduced density range $0 < \rho_r < 2$. The observed strong redshift of the band center, the intensity enhancement, and the band shape distortion all indicate the presence of an attractive interaction between ethanol and CO_2. An analysis based on the analytical Buckingham−Ben-Amotz model indicates that the frequency shift is strongly dominated by the attractive, rather than by the repulsive, forces and that this attractive contribution arises almost entirely from the dispersion interactions. The deviation of the experimentally observed shifts from the theoretically predicted linear behavior expected in a homogeneous fluid as a function of pressure (in the mean-field approximation) strongly suggests the existence of local density enhancements and was therefore used to estimate empirical local density enhancement factors as a function of density. Differences between these local density-enhancement factors, extracted from the OD vibrational shift, and those extracted from NMR data are rationalized on the basis of the observation that IR spectra probe the solvent density over a shorter range than do the NMR spectra. It is subsequently argued that the larger local densities extracted from the IR spectra are consistent with the presence of a very local, likely spatially asymmetric, enhancement in the number of CO_2 molecules near the ethanol solute, and, most probably, near the OD group. This explanation is consistent with the observation of local density enhancements in the IR spectra up to unusually high temperatures, $T_r \geq 1.3$, which itself suggests the presence of a relatively strong attractive interaction between ethanol and CO_2. These arguments are supported by ab initio calculations of an ethanol−CO_2 complex, which reveal the presence of a relatively strong, specific OH−CO_2 interaction. This calculated result also confirms the origin of the redshift and intensity enhancements observed experimentally for the ν_{OD} mode and shows that the stabilization of the ethanol−CO_2 complex is due to the EDA interaction between the carbon atom of CO_2 and the oxygen atom of the hydroxyl group.

Acknowledgment. Susan Tucker is pleased to thank the Ministère de la Recherche for the Senior Scientist Fellowship Grant under the auspices of which this work has been completed.

References and Notes

(1) Orville-Thomas, W. J.; Yarwood, J. *Molecular Liquids: Dynamics and Interactions*; D. Reidel Publishing Company: Dordrecht, Holland, 1984; Vol. 135.

(2) *Supercritical Fluids: Fundamentals and Application*; Kiran, E., Debenedetti, P. G., Peters, C. J., Eds.; Kluwer Academic Publishers: Dordrecht, 2000; Vol. 366.

(3) Tucker, S. C. *Chem. Rev.* **1999**, *99*, 391.

(4) Kajimoto, O. *Chem. Rev.* **1999**, *99*, 355.

(5) Perrut, M.; Reverchon, E. Particle Design−Materials and Natural Products Processing. *Proceedings of the 7th Meeting on Supercritical Fluids*; Vandoeuvre: Antibes, France, 2000; INPL 54501.

(6) Nishikawa, K.; Morita, T. *Chem. Phys. Lett.* **2000**, *316*, 238.

(7) Egorov, S. A. *J. Chem. Phys.* **2000**, *112*, 7138.

(8) Egorov, S. A. *J. Chem. Phys.* **2000**, *113*, 7502.
(9) Song, W.; Biswas, R.; Maroncelli, M. *J. Phys. Chem. A* **2000**, *104*, 6924.
(10) Maddox, M. W.; Goodyear, G.; Tucker, S. C. *J. Phys. Chem. B* **2000**, *104*, 6248.
(11) Goodyear, G.; Maddox, M. W.; Tucker, S. C. *J. Chem. Phys.* **2000**, *112*, 10327.
(12) Pratt, L. R.; Chandler, D. *J. Chem. Phys.* **1976**, *65*, 2925.
(13) Oxtoby, D. W. *Adv. Chem. Phys.* **1979**, *40*, 1.
(14) Schweizer, K. S.; Chandler, D. *J. Chem. Phys.* **1982**, *76*, 2296.
(15) Rey, S.; Cansell, F. *Polymer J.* **1998**, *30*, 863.
(16) Rey, S. Fractionnement du poly(oxyde d'éthylène) et du polystyrène avec le mélange supercritique universel CO_2−ethanol. Approche du comportement microscopique et thermodynamique de ces systèmes. Ph.D. Thesis, Bordeaux I, 1999.
(17) McHugh, M. A.; Krukonis, V. J. *Encyclopedia of Polymer Science and Engineering* **1989**, *16*, 368.
(18) Ben-Amotz, D.; Herschbach, D. R. *J. Phys. Chem.* **1993**, *97*, 2295.
(19) Ben-Amotz, D.; Lee, M. R.; Cho, S. Y.; List, D. J. *J. Chem. Phys.* **1992**, *96*, 8781.
(20) Buckingham, A. D. *Proc. R. Soc. London, Ser. A* **1958**, *248*, 169.
(21) Fulton, J. L.; Yee, G. G.; Smith, R. D. *J. Am. Chem. Soc.* **1991**, *113*, 8327.
(22) Fulton, J. L.; Yee, G. G.; Smith, R. D. Hydrogen bonding in simple alcohols in supercritical fluids: an ftir study. In *Supercritical fluid engineering science: Fundamental and applications*; Kiran, E., Brennecke, J. F., Eds.; Washington, DC, 1993; Vol. 514, p 175.
(23) Tassaing, T.; Lalanne, P.; Rey, S.; Cansell, F.; Besnard, M. *Ind. Eng. Chem. Res.* **2000**, *39*, 4470.
(24) Reilly, J. T.; Bokis, C. P.; Donohue, M. D. *Int. J. Thermophys.* **1995**, *16*, 599.
(25) Hemmaplardh, B.; King, A. D., Jr. *J. Phys. Chem.* **1972**, *76*, 2170.
(26) Gupta, S. K.; Lesslie, R. D.; King, A. D., Jr. *J. Phys. Chem.* **1973**, *77*, 2011.
(27) Jamroz, M. H.; Dobrowolski, J. C.; Bajdor, K.; Borowiak, M. A. *J. Mol. Struct.* **1995**, *349*, 9.
(28) Danten, Y.; Tassaing, T.; Besnard, M. *J. Phys. Chem. A.* **2002**, *106*, 11831.
(29) Cox, A. J.; Ford, T. A.; Glasser, L. *J. Mol. Struct.* **1994**, *312*, 101.
(30) Zhang, N. R.; Shillady, D. D. *J. Chem. Phys.* **1994**, *100*, 5230.
(31) Melendez Pagan, Y.; Ben-Amotz, D. *J. Phys. Chem. B* **2000**, *104*, 7858.
(32) Ben-Amotz, D.; Herschbach, D. R. *J. Phys. Chem.* **1990**, *94*, 1038.
(33) Inskeep, R. G.; Kelliher, J. M.; McMahon, P. E.; Somers, B. G. *J. Chem. Phys.* **1958**, *28*, 1033.
(34) Egorov, S. A.; Skinner, J. L. *J. Phys. Chem. A* **2000**, *104*, 483.
(35) Egorov, S. A.; Yethiraj, A.; Skinner, J. L. *Chem. Phys. Lett.* **2000**, *317*, 558.
(36) Lu, J.; Han, B.; Yan, H. *Phys. Chem. Chem. Phys.* **1999**, *1*, 3269.
(37) Eckert, A.; Ziger, D. H.; Johnston, K. P.; Ellison, T. K. *Fluid Phase Equilib.* **1983**, *14*, 167.
(38) Wada, N.; Saito, M.; Kitada, D.; Smith, R. L.; Inomata, H.; Arai, K.; Saito, S. *J. Phys. Chem. B* **1997**, *101*, 10918.
(39) Urdahl, R. S.; Mayers, D. J.; Rector, K. D.; Davis, P. H.; Cherayil, B. J.; Fayer, M. D. *J. Chem. Phys.* **1997**, *107*, 3747.
(40) Ikawa, S.; Fujita, Y. *J. Phys. Chem.* **1993**, *97*, 10607.
(41) The one vibrational study in compressible SCFs that does not exhibit such nonlinear deviations was performed in neat supercritical ethane rather than on an attractive solute−solvent system.[52] As shown by Egorov and Skinner,[34] the neat Lennard-Jones SCF in three dimensions is anomalous in that it exhibits negligible potential-induced[10] LDE effects. Consequently, it is not surprising that in neat supercritical ethane, which might reasonably well be modelled as a 3D Lennard-Jones fluid, no significant nonlinearity, and thus no evidence for LDEs, was observed.
(42) Goodyear, G.; Tucker, S. C. *J. Chem. Phys.* **1999**, *110*, 3643.
(43) Kanakubo, M.; Aizawa, T.; Kawakami, T.; Sato, O.; Ikushima, Y.; Hatakeda, K.; Saito, N. *J. Phys. Chem. B* **2000**, *104*, 2749.
(44) Heitz, M. P.; Maroncelli, M. *J. Phys. Chem. A* **1997**, *101*, 5852.
(45) Luo, H.; Tucker, S. C. *J. Phys. Chem. B* **1997**, *101*, 1063.
(46) Inomata, H.; Saito, S.; Debenedetti, P. *Fluid Phase Equilib.* **1996**, *116*, 282.
(47) Iwai, Y.; Koga, Y.; Arai, Y. *Fluid Phase Equilib.* **1996**, *116*, 267.
(48) Frisch, M. J.; Trucks, G. W.; Schlegel, H. B.; Gill, P. M. W.; Johnson, B. G.; Robb, M. A.; Cheeseman, J. R.; Keith, T.; Petersson, G. A.; Montgomery, J. A.; Raghavachari, K.; Al-Laham, M. A.; Zakrzewski, V. G.; Ortiz, J. V.; Foresman, J. B.; Cioslowski, J.; Stefanov, B. B.; Nanayakkara, A.; Challacombe, M.; Peng, C. Y.; Ayala, P. Y.; Chen, W.; Wong, M. W.; Andres, J. L.; Replogle, E. S.; Gomperts, R.; Martin, R. L.; Fox, D. J.; Binkley, J. S.; Defrees, D. J.; Baker, J.; Stewart, J. P.; Head-Gordon, M.; Gonzalez, C.; Pople, J. A. *Gaussian 94*, Gaussian, Inc.: Pittsburgh, PA, 1995.
(49) Boys, S. F.; Bernardi, F. *Mol. Phys* **1970**, *19*, 553.
(50) Bondi, A. *J. Phys. Chem.* **1964**, *68*, 441.
(51) Gray, C. G.; Gubbins, K. E. *Theory of molecular fluids Volume 1: Fundamentals*; Clarendon Press: Oxford, 1984.
(52) Ben-Amotz, D.; LaPlant, F.; Shea, D.; Gardecki, J.; List, D. J. In *Supercritical Fluid Technology*; Bright, F. V., McNally, M. E., Eds.; ACS Symposium Series 488; American Chemical Society, Washington, 1992.